Simple model for the stripe phase in compounds with bent-core molecules which exhibit a lower-temperature ferroelectric smectic-*A* phase

N. V. Madhusudana [*]

Raman Research Institute, C. V. Raman Avenue, Bengaluru-560080, India

Bent-core (BC) molecules usually exhibit polar packing in smectic layers in which the long or bow axes tilt with respect to the layer normal. In many compounds, the tilt angle goes to zero, and typically the polarization (**P**) of neighboring layers has an antiferroelectric order (SmAP_{AF}). A careful molecular engineering has led to the discovery of the ferroelectric SmAP_F phase in a few BC compounds. Detailed experimental studies [Zhu *et al.*, J. Am. Chem. Soc. **134**, 9681 (2012)] have shown that one of the compounds undergoes a weak first order transition to a striped phase (SmAP_{Fmod}), in which the repolarization switching occurs at a *threshold* electric field, the latter increasing with temperature. The main optical birefringence of the SmAP_{Fmod} phase increases rapidly with the field at lower temperatures of its range. A small ($<10\%$) fraction of the BC molecules can be expected to have less bent conformations in excited states (ESs), and we argue that the ES conformers rotate freely about the bow axes, and aggregate to form regions without any polar order to gain rotational entropy. In turn, a favorable div**P** term leads to the formation of stripes in the polarized regions made of ground state conformers. Based on this physical picture, we develop a simple phenomenological model to reproduce all the experimental trends qualitatively. In sample cells with insulating layers neighboring stripes prefer to have an antiparallel orientation of the mean **P** direction. The dielectric constant of the stripe phase increases with a dc bias electric field, a trend which is opposite to that in other ferroelectric liquid crystals.

DOI: 10.1103/PhysRevE.100.022706

I. INTRODUCTION

Smectic-*C* liquid crystals have a layered arrangement of tilted molecules with shape anisotropy. The layers can exhibit an in-plane polarization if the rodlike molecules are chiral [1], or the molecules have bent cores (BCs) which pack with a polar order [2] and the layer itself in turn develops chirality [3]. A more symmetric structure results if the molecules do not tilt, and the polarized smectic-*A* layers do not develop chirality. Several such examples are known [4–7], but most of them have an antiferroelectric order of neighboring layers (SmAP_{AF} phase). This is to be expected, as (i) such a structure is favored entropically due to the ease of fluctuations of the BC molecules between neighboring layers, and (ii) the main electrostatic interaction between the layers results from the polarization charge densities due to thermal fluctuations of the **P** field, which always favors the antiferroelectric order [8,9]. By coupling bulky carbosilane end groups to the hydrocarbon chains of the BC molecules, the Boulder group has discovered the ferroelectric SmAP_F phase, which has the highest symmetry of all the known ferroelectric liquid crystal phases [10–12]. The bulky carbosilane end groups prevent interlayer fluctuations of the BC molecules. Further, as they have a higher dielectric constant than the hydrocarbon chain, they can effectively screen the electrostatic interlayer interaction.

The smectic layers are fluid, which allows the development of a div**P** type distortion in the ferroelectric phase. Usually, this is just a surface term, which can be ignored in most cases. However, by including the term $\mathbf{P}^2 \text{div}\mathbf{P}$ and allowing the magnitude of **P** to vary spatially, early theoretical studies predicted that the paraelectric phase undergoes a transition to modulated phases in which unit cells with either hexagonal or stripe structure are separated by walls at which the **P** vector of reduced magnitude changes its orientation rapidly [13–15]. The domain size is predicted to diverge as the modulated to uniform phase transition point is approached.

The first examples of phases with polarization modulation in the *bulk* were found in compounds made of BC molecules, with smectic-*C* type layers [16–18]. In the B_7 phase, in a given layer, splay modulation of polarization occurs in stripes with a width of a few tens of nanometers, the tilt orientation itself changes sign between successive stripes, and the magnitude of tilt angle goes to zero at the walls between stripes. This in turn leads to a spatial undulation of the layers, and the resulting structure gives rise to very complex and beautiful textures. In the B_1 phase, the change in the tilt orientation is accommodated by a shift of successive stripes by half the layer spacing, generating a rectangular symmetry in the structure [18]. A phenomenological model for the B_7 phase was subsequently developed, in which a coupling between the tilt and div**P** was *necessary* for the formation of the modulated phase [19,20]. As such, in this model a modulated phase is not expected to be exhibited in Sm*A* liquid crystals whose layers do not have tilted molecules. Nevertheless, detailed experimental studies on a compound with BC molecules by the Boulder group have uncovered a polarization splay-modulated phase with nontilted molecules (SmAP_{Fmod}) [21].

[*]nvmadhu@rri.res.in

The compound exhibits a first order transition from the isotropic phase to the modulated phase (SmAP_{Fmod}), which has a temperature range of over 30 K. It undergoes a transition to the uniform SmAP_F phase in a weakly first order transition. The main characteristics of the modulated phase are a very weak in-layer optical anisotropy (biaxiality), and a polarization reversal peak exhibited at a *threshold* electric field, which increases from a finite value as the temperature is increased from the transition to the uniform (SmAP_F) phase. At lower temperatures of the SmAP_{Fmod} phase the main optical birefringence corresponding to the anisotropy between the layer normal and the in-plane direction perpendicular to the applied field increases rapidly above some field and saturates near that exhibited by the SmAP_F phase. At higher temperatures, the birefringence does not exhibit the rapid rise at the fields applied. In the uniform phase the polarization current peak occurs at zero field, corresponding to the V-shaped switching discussed earlier by the Boulder group [22]. The first order nature of the transition between the two ferroelectric phases is also evidenced by a coexistence of the two types of current peaks over a temperature range of ∼8 K. The magnitude of polarization in the modulated phase is smaller than that in the uniform phase, with the ratio decreasing from ∼0.7 to ∼0.5 as the temperature is increased. Freeze fracture electron microscopy has been used to directly visualize the stripes of a width ∼20 nm. Small angle x-ray studies showed a few peaks, with the largest spacing corresponding to the above stripe width. However, the other peaks could not be indexed to a rectangular lattice. The authors suggested that the different peaks may signify that the stripe width may depend on the curvature of the layers in the focal conic domains of the powder sample used in the x-ray studies. Assuming that the magnitude of polarization does not depend on temperature, the low value of the in-layer biaxiality and large value of **P** could be understood if the splay angle varied from $-\pi/2$ to $+\pi/2$ between the walls of the stripe. The authors argued that the bistability of the SmAP_{Fmod} structure could arise from a polar anchoring at the cell surfaces, which in turn would generate both surface and bulk defects, and a strong electric field would expel one pair of defects from the liquid crystal, latching the structure. They used an elastic model with both polar and nonpolar anchoring energies of the **P** vector at the walls of the stripe to calculate the electric field dependence of the birefringence. In order to account for the different trends at high and low temperatures mentioned above, the effective elastic constant had to be increased by ∼40 times as the temperature was increased by ∼20 K. This was attributed to an increase in the screening length as ions would be more readily swept from the sample by the field at higher temperatures.

Our aim in this paper is to develop a phenomenological model for the SmAP_F to SmAP_{Fmod} transition, and to calculate the temperature dependences of the threshold field and the field dependence of birefringence measured in the experiment. We also present other parameters like the biaxiality, stripe width, etc., which are predicted on the basis of the model. The model is based on a few assumptions, and to motivate the most important one, we briefly describe some properties of nematic (*N*) liquid crystals made of BC molecules. In the *N* phase, the molecules have to rotate relatively freely about their bow axes, which requires that the opening angle between the two arms of the BC molecule has to be larger than ∼140° or so. A variety of experimental studies on many such compounds [23] has established that the medium is *not homogeneous*, but consists of *clusters* made of ∼100 molecules which have a local arrangement of Sm*C* type short range order. The cluster size is not very sensitive to temperature variations, but can persist well into the higher-temperature isotropic phase. We have shown in a recent paper [24] that the BC molecules which usually have two or more ester linkage groups in their aromatic cores are not highly rigid, but exhibit conformational variety. In particular ∼10% of the molecules are in an excited state (ES) in which the opening angle is larger than average, with a smaller moment of inertia about the bow axes. The ES molecules can approach each other more closely than in the ground state (GS) conformers which are more bent, and the increased strength of the London dispersion interaction leads to the formation of a layered arrangement, as the effective smectic to nematic transition point is enhanced compared to that of the GS molecules. Based on this physical picture, we developed a phenomenological model for the nematic with clusters, and accounted for several experimental results like a significant enhancement in the magnetic-field-induced (paranematic to nematic) critical point compared to that in compounds without clusters [25], etc. More recently, we have found that those clusters which are close to the surface of the cell can organize themselves to change the anchoring conditions quasiperiodically, leading to a self-decoration of the orientational field of the BC nematic [26]. This observation also implies that the clusters of ES conformers are long lived. In short, the ES conformers of BC molecules can condense together to give rise to a nonuniform structure even in the fluid nematic phase. In the next section we will make use of this observation in developing a phenomenological model for the SmAP_{Fmod} phase, and its transition to the uniform SmAP_F phase.

II. THEORETICAL MODEL

Both SmAP_F and SmAP_{Fmod} phases have polarized layers, and we assume that a second order paraelectric to ferroelectric transition occurs in the Sm*A* layers at a transition temperature T^*, and is described by the simplest version of the Landau theory with temperature dependent quadratic and temperature independent quartic terms in the polar vector order parameter **m**, whose magnitude is $\langle \cos\theta \rangle$, the statistical average of the projections of unit vectors along the arrow axes of the BC molecules on **m** (see Fig. 1). The polarization is then given by $\mathbf{P} = p\mathbf{m}$, where p is the magnitude of **P** when **m** is saturated. In the compound studied in Ref. [21], the isotropic phase undergoes a first order transition directly to the SmAP_{Fmod} phase, which means that T^* lies well above that transition temperature. In view of the observations of the previous paragraph, we propose that a small fraction (say ∼10%) of the molecules have ES conformations, which are less bent than the GS conformers, and can freely rotate about their bow axes, and hence do not contribute to **P**. The ES conformers can in turn aggregate to gain rotational entropy, and form unpolarized Sm*A* type clusters. It is interesting to note that in the nematic phase the clusters of ES conformers have a lower local symmetry compared to the medium as a
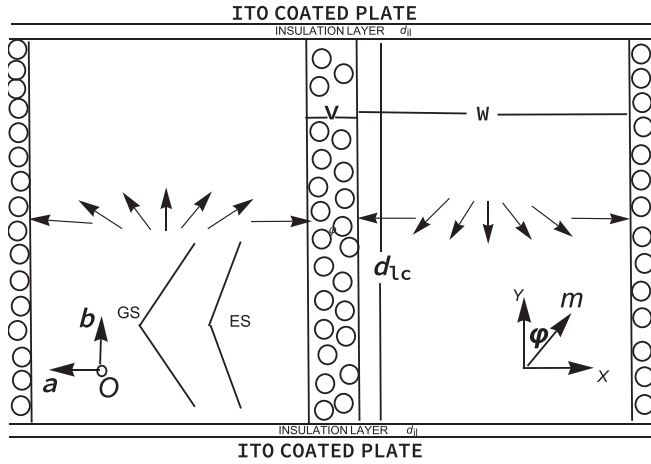
FIG. 1. Schematic diagram of a cell filled with liquid crystal in the SmAP_{Fmod} (stripe) phase. The outer indium-tin-oxide (ITO) coated plates have a thickness of ~ 1 mm, the insulating layer a thickness of $d_{il} \sim 10$ nm, and the cell gap a thickness of $d_{lc} \sim 10 \, \mu$m. The smectic-A layers are stacked parallel to the plane of the page, with the layer normal along the z axis. The splayed structures of the polar order $\boldsymbol{m}$ exhibited by the more strongly bent ground state (GS, lower left) BC molecules, and described by the angle φ between $\boldsymbol{m}$ and the Y axis, have opposite configurations in adjacent stripes of a rested sample, with the applied electric field $= 0$, implying that the *polar* anchoring of $\boldsymbol{m}$ at the insulating layer is negligible. The less bent excited state (ES) conformers indicated by circles can rotate freely, and aggregate to form walls of width v (~ 1 or 2 nm) between the polar stripes of width w (approximately tens of nanometers). $\boldsymbol{m}$ is orthogonal to the interface with the walls made of ES molecules, implying a strong anchoring at that interface. The small angle x-ray Bragg peak corresponds to $v + w$. The molecular frame is described by the arrow $(-a)$ axis, the bow $(-b)$ axis, and the o axis orthogonal to the molecular plane.

whole, while in the polarized SmA layers the clusters have a *higher* local symmetry. The polarization vector of the medium outside the cluster would preferentially align perpendicular to the interface, and we assume in the following that **P** points towards the interface. The relevant interfacial tension is denoted by Γ. The polarized interface in turn costs a positive self-energy of the medium, and in the liquid layer this can be reduced by the allowed div$\boldsymbol{m}$ (splay) distortion of the $\boldsymbol{m}$ field. We assume that the medium favors the *positive* sign of this distortion. The distortion costs a curvature elastic energy, and further, as div**P** is equivalent to polarization charge density, there is a positive long range Coulomb energy cost between the charge densities. The medium usually has ionic impurities which can screen this interaction to some extent. Earlier experimental and theoretical [27–30] studies on SmC^* liquid crystals have shown that the Coulomb interaction effectively enhances the splay elastic constant but the additional contribution is proportional to $1/q^2$, where q is the wave vector of the distortion. Consequently, while the structure of small circular drops of the polarized SmC^* layers is hardly affected, larger drops with diameters of a few tens of micrometers avoid splay distortion of the **P** field [29,30]. In the experimental system exhibiting the SmAP_{Fmod} phase [21], and in our model, the distortion is limited to a length scale of a few tens of

nanometers, and the splay elastic constant is not significantly enhanced. However, we will argue that the Coulomb energy can make an important contribution to the $\mathbf{m}^2$div$\mathbf{m}$ term [13–15] which will be included in the model.

It is convenient to have a pictorial representation (Fig. 1) of the structure of the modulation before writing the relevant free energy expression. The liquid crystal is supposed to be made of smectic layers parallel to the plane of the page, with the layer normal along the z axis. The splayed structure is the same as that proposed in Ref. [21], the unique feature being that the walls are made of thin regions extended along the y axis populated by BC molecules with ES conformation rotating relatively freely about the bow axes (oriented along the layer normal), and symbolically shown as circles in the figure. Between two such walls, the polarized medium with GS conformers has a splay-bend distorted $\mathbf{m}$ field, the azimuthal angle $\varphi(x)$ measured from the y axis (which points vertically upwards in Fig. 1) increasing from $-\pi/2$ at $x = -w/2$ to $+\pi/2$ at $x = +w/2$, where w is the width of the stripe, and we refer to the stripe on the left side of Fig. 1, in which $\mathbf{m}$ is pointed along the positive y axis on average. As we shall see w is of the order of a few tens of nanometers. The width (v) of a SmA wall can be expected to be much smaller, ~ 1 or 2 nm. The stripe width measured by x-ray scattering is $w + v$. In Fig. 1, we have shown two adjacent stripes, the one on the right being antiparallel to the one on the left. We shall discuss this aspect later. It may be noted that as the ES conformers are less bent than the GS conformers, the layer spacing in the SmA walls can be expected to be slightly larger than in the polarized domains between the walls, and this may be the origin of the slightly undulated structure seen by freeze fracture electron microscopy [21]. A dc electric field $\mathbf{E}_{\mathbf{lc}}$ acts along the y axis. With $m = |\mathbf{m}|$, the free energy density at a given position x within the stripe can now be written as

$$
\begin{aligned}
F(x) = &\frac{a}{2}(T - T^*)m^2 + \frac{b}{4}m^4 - \alpha \big(m_s^2 - m^2\big)\text{div}\boldsymbol{m} \\
&+ \frac{\beta}{2}[(\text{div}\boldsymbol{m})^2 + (\boldsymbol{m} \times \text{curl}\boldsymbol{m})^2] \\
&+ \frac{(p\,m_x)^2}{2\varepsilon_0\varepsilon} - pm_y E_{lc}.
\end{aligned}
\tag{1}
$$

In the above equation, a and b are the usual Landau coefficients, the αm_s^2 term favors a positive div$\boldsymbol{m}$ distortion, and the m^2div$\boldsymbol{m}$ term, which is allowed by the symmetry of the system [13–15], opposes the div$\boldsymbol{m}$ distortion. Assuming an infinite sample extending in all directions, it is clear that the net charge density in each stripe is zero, and there is no Coulomb interaction between the stripes. In any case, we do not consider interstripe interactions in this paper. However, interaction of the polarization charges from the div$\boldsymbol{m}$ distortion within the stripe can generate a residual positive energy, which contributes to the m^2div$\boldsymbol{m}$ term in the equation. It is clear that as long as $m^2 < m_s^2$, the third term above gives rise to the favored div$\boldsymbol{m}$ distortion. For the sake of simplicity, we assume $m_s = 1$ in all our calculations, to discount the possibility of a reentrant phase with a negative div$\boldsymbol{m}$ distortion at low temperatures. We use a one-elastic constant ($=\beta$) approximation-for describing both the splay and bend distortions of $\boldsymbol{m}$. The last-but one term is the polarization self-energy, with ε_0 being the vacuum

dielectric constant and ε the relative dielectric constant of the SmA phase, without the contribution from the spontaneous polarization. The last term is the $-\mathbf{P} \cdot \mathbf{E}_{\mathbf{lc}}$ term, arising from the action of an external field on the medium. In the uniform phase without stripes (SmAP_F), only the first two terms and the last term are relevant. In the following, we use "uniform" and "SmAP_F" interchangeably, as also the terms "SmAP_{Fmod}" and "stripe."

As mentioned above, the transition from SmAP_F to SmAP_{Fmod} is assumed to occur far below T^*, allowing us to assume that the magnitude m is fixed across the stripe. We can then rewrite Eq. (1) using the azimuthal angle φ as follows:

$$F(x) = \frac{a}{2}(T - T^*)m^2 + \frac{b}{4}m^4 - \alpha(m_s^2 - m^2)m \cos\varphi \frac{d\varphi}{dx}$$
$$+ \frac{\beta m^2}{2}\left(\frac{d\varphi}{dx}\right)^2 + \left(\frac{p^2 m^2}{2\varepsilon_0 \varepsilon}\right)\sin^2\varphi - pmE_{lc}\cos\varphi. \quad (2)$$

We first consider the problem in the absence of the electric field ($E_{lc} = 0$). Making use of the symmetry of the stripe structure about the midpoint ($x = 0$), the Euler-Lagrange equation with respect to φ yields the following equation for the stripe width w:

$$w = 2\,\xi \int_0^{\pi/2} \frac{d\varphi}{\sqrt{C_0 + \sin^2\varphi}}, \quad (3)$$

where $\xi = (\beta\varepsilon_0\varepsilon)^{0.5}/p$ is the length over which the elastic distortion lowers the polarization self-energy. The integration constant C_0 in Eq. (3) determines the stripe width w. The α term with a linear dependence on div$\boldsymbol{m}$ has no influence on the φ profile across the stripe, or on the stripe width w, as we assume a *fixed* boundary condition with $\mathbf{P}$ strongly anchored along the normal to the interface (Fig. 1). However, it does affect the magnitude of the order parameter m, and hence the free energy. The free energy per unit volume *averaged* over the stripe width takes the following form:

$$\bar{F} = \frac{a}{2}(T - T^*)m^2 + \frac{b}{4}m^4 - \frac{2}{w}\alpha(m_s^2 - m^2)m + \frac{2\gamma m^2}{w}$$
$$+ \frac{\beta m^2}{\xi}\left(\frac{C_0}{2\xi} + \frac{2}{w}\int_0^{\pi/2}\frac{\sin^2\varphi \, d\varphi}{\sqrt{C_0 + \sin^2\varphi}}\right), \quad (4)$$

where we have included the interfacial energy cost, and used the mean field result that $\Gamma = \Upsilon m^2$. The above free energy density can now be minimized with respect to both the order parameter m and the stripe width w to find their equilibrium values at a given relative temperature ($T - T^*$). We use the following parameters in MKS units: $a = 10^4 \, J/(m^3 \, K)$, $b = 1.4 \times 10^6 \, J/m^3$, $\alpha = 55 \, 10^{-5} \, J/m^2$, $\beta = 2.5 \, 10^{-12} \, J/m$, $\Upsilon = 10^{-5} \, J/m^2$, and $\varepsilon_0\varepsilon = 4 \times 10^{-10}$. The dielectric constant of the SmA phase is assumed to be $\sim$40, as the GS molecules would exhibit a short range polar order with a few aligned molecules even in the isotropic phase. The iterative procedure for minimizing the free energy given by Eq. (4) is to assume some value of C_0, calculate w, minimize the free energy with respect to the order parameter (m), and adjust C_0 to get the absolute minimum of the free energy. The calculations were made using *Mathematica 11*. This minimized free energy has to be compared with that of the uniform phase (SmAP_F),

which is given by

$$F_u = -\frac{a^2}{4b}(T^* - T)^2, \quad (5)$$

with the equilibrium value of the order parameter $m_u = [a(T^* - T)/b]^{0.5}$. At low temperatures, the uniform phase has a lower free energy and is the stable phase. As the temperature is raised to $T^* - T \approx 85.3 \, K$, the free energy of the stripe phase becomes lower than that of the uniform phase. The order parameter jumps down from $m_u = 0.7806$ to $m = 0.7621$, in a weak first order transition. The corresponding heat of transition is given by $\Delta H = aT_{tr}(m_u^2 - m^2)/2$. Assuming $T^* = 500 \, K$, the stripe to uniform transition temperature $T_{tr} = 414.7 \, K$, and the heat of transition is $\approx 6 \times 10^4 \, J/m^3$. If the molecular weight of the BC mesogen is about 1000, this corresponds to about 60 J/mol, which is similar to the value estimated by differential scanning calorimetry in Ref. [21]. Though the jump in the order parameter is quite small, in view of the very different dispositions of the $\boldsymbol{m}$ fields in the two phases, the polarization shows a much bigger jump. Assuming $p = 3.5 \times 10^{-3} \, C/m^2$, the polarization in the uniform phase ($P_u = pm_u$) is $2.73 \times 10^{-3} \, C/m^2$ at T_{tr}. The polarization averaged over the stripe width w is given by

$$P = \frac{2\,p\,m\,\xi}{w} \int_0^{\pi/2} \frac{\cos\varphi \, d\varphi}{\sqrt{C_0 + \sin^2\varphi}}, \quad (6)$$

which is $2.09 \times 10^{-3} \, C/m^2$ at T_{tr}, a value considerably lower than that of the uniform phase. The stripe width is $\sim$56 nm at T_{tr}, but decreases rapidly to $\sim$25.7 nm at $T^* - T = 65 \, K$, with m going down to $\sim$0.681 and P to $1.53 \times 10^{-3} \, C/m^2$. These numbers are comparable to the experimental values [21]. The temperature variations of m, the reduced polarization P/p, and the reduced stripe width $w(T)/w(T_{tr})$, are shown in Fig. 2. The variations of the azimuthal angle φ with the reduced x coordinate ($2x/w$) across half the symmetric structures of the stripes are shown in Fig. 3 at three temperatures.

III. RESULTS WITH DC ELECTRIC FIELD

Experimentally, polarization is measured by applying a low-frequency triangular electric field $\mathbf{E}$ to the sample, and the area of the current peak arising from the reorientation of $\mathbf{P}$ after the sign reversal of $\mathbf{E}$ is a measure of P. In the low-temperature SmAP_F (uniform) phase, the peak is centered at $E = 0$ [21], showing that the $\mathbf{P}$ vector is aligned parallel to the cell walls when $\mathbf{E} = 0$. This means that the polar anchoring at the cell surfaces is overwhelmed by the polarization self-energy, unlike in another compound with BC molecules in which the polar anchoring is the dominant interaction in the SmAP_F phase [10]. The important role played by the insulating layers at the walls of the liquid crystal cell in systems, in which the repolarization peak is centered at $E = 0$, has been elucidated in detail by the Boulder group [22,31]. In our theoretical analysis on the SmAP_{Fmod} (stripe) phase, we will simply assume an electric field $\mathbf{E}_{\mathbf{lc}}$ to be acting in the bulk, and make some remarks on the effect of the insulating layers in actual experimental cells later. $\mathbf{E}_{\mathbf{lc}}$ is supposed to be acting along the positive y axis (Fig. 1), and the average polarization vectors of all the stripes are assumed to be oriented along
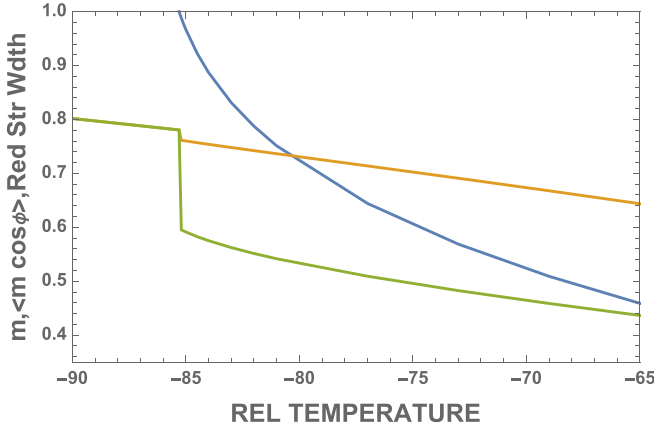
FIG. 2. Calculated variations of the order parameter m (topmost curve near relative temperature $T - T^* = -65$ K) and spatially averaged projection of m along the y axis ($\langle m \cos \varphi \rangle$, bottom-most curve near $T - T^* = -65$ K) across the SmAP_{Fmod} (stripe) to SmAP_{F} (uniform) phase transition at $T_{tr} - T^* = -85.3$ K. The order parameter m exhibits a small jump in a thermodynamically weak transition, but the polarization $\mathbf{P}$ ($= p \langle m \cos \varphi \rangle$, $p = 3.5 \times 10^{-3}$ C/m^2) exhibits a large jump due to the change in the spatial distribution of m. The reduced stripe width $[w(T)/w(T_{tr})]$ is shown in the middle curve, where $w(T_{tr})$ (the stripe width at T_{tr}) = 56 nm.

the same direction, i.e., $\mathbf{P_{av}} \| \mathbf{E_{lc}}$ in the poled sample. Using Eq. (2), the Euler-Lagrange equation with respect to φ now leads to the following relation for the stripe width:

$$w_{ep} = 2\,\xi \int_0^{\pi/2} \frac{d\varphi}{\sqrt{C_{ep} - \xi_r^2 \cos\varphi + \sin^2\varphi}}, \qquad (7)$$

where the dimensionless parameter $\xi_r = \xi / \xi_{ep}$, with $\xi_{ep} = [\beta m_{ep}/(2pE_{lc})]^{0.5}$, the length over which the elastic distortion relaxes the electric energy of P due to E_{lc}. The suffix ep stands for positive electric field. We can now use this relation in
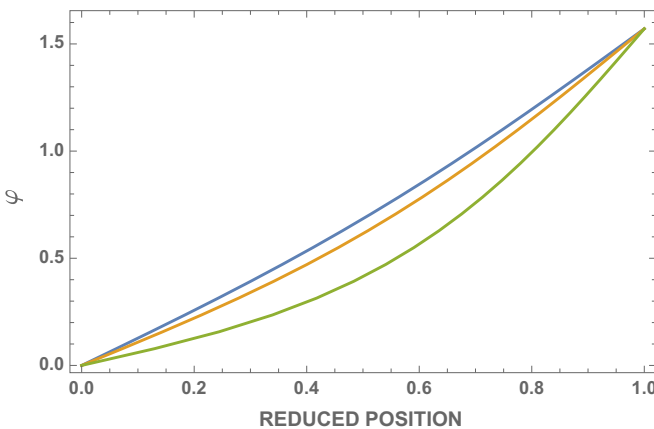

FIG. 3. Variation of φ, the angle made by m with the y axis (in the symmetric configuration of a stripe in the left half of Fig. 1) with the reduced position $2x/w(T)$. The relative temperatures $(T - T^*)$ are -65 K (topmost curve, $w = 25.7$ nm), -75 K (middle curve, $w = 33.8$ nm), and -85 K (bottom-most curve, $w = 54.1$ nm). The φ angle lingers close to 0 over a larger fraction of the stripe at a lower temperature.

Eq. (2) to calculate the free energy density $\langle F_{ep} \rangle$, averaged over the stripe width w_{ep}. As before, at any given positive E_{lc}, we can find the absolute minimum of this free energy with respect to both m_{ep} and w_{ep} by using an iterative procedure, noting that ξ_r itself depends on m_{ep}. The main results are that the order parameter, stripe width, the polarization averaged over the stripe width, and the transition temperature T_{tr} are all enhanced compared to their field-free values. Optical anisotropy is a very useful property to characterize the molecular arrangement in liquid crystalline phases, and has been used to study the SmAP_{Fmod} phase [21]. BC molecules are biaxial, with the optical polarizability along the bow axis having the highest value, that along the arrow axis having a lower value, and the one along the normal to the molecular plane having the lowest value. In a perfectly ordered SmAP_{F} phase at a very low temperature, the corresponding (saturated) refractive indices are denoted by n_{bs}, n_{as}, and n_{os} respectively. For the sake of simplicity, we assume that the bow axes, which are aligned normal to the SmA layers in both phases being discussed, have a perfect orientational order. This means that for a light beam traversing in the plane of the layers, and polarized along the z axis, n_{bs} is the refractive index independent of temperature. As the order parameter m is not saturated, the principal in-plane refractive indices for polarization of the light beam along and perpendicular to m can be calculated as 2D averages:

$$n_a = \sqrt{0.5\left[n_{as}^2(1 + m^2) + n_{os}^2(1 - m^2)\right]},$$
$$n_o = \sqrt{0.5\left[n_{as}^2(1 - m^2) + n_{os}^2(1 + m^2)\right]}. \qquad (8)$$

As the maximum stripe width is about 10 times smaller than a typical wavelength in the visible region, the in-plane optical response can be calculated as an appropriate average over the width of the stripe. For a light beam propagating along the layer normal (z axis, see Fig. 1), the biaxiality is given by

$$\delta n = n_y - n_x = (n_a - n_o)\langle \cos 2\varphi \rangle. \qquad (9)$$

For light propagating along the y axis and polarized in the layer plane, the effective refractive index is given by

$$n_x = n_{ef} = \frac{n_a n_o}{\sqrt{(n_a^2 - n_o^2)\langle \cos^2 \varphi \rangle + n_o^2}}. \qquad (10)$$

The triangular brackets in Eqs. (9) and (10) signify averaging over the width of the stripe. The main birefringence for light propagating along the y axis is given by $\Delta n = n_z - n_x = n_{bs} - n_{ef}$. In our calculations, we have used the following values for the saturated refractive indices: $n_{bs} = 1.65$, $n_{as} = 1.57$, and $n_{os} = 1.53$. In the uniform phase, $\delta n = n_a - n_o$ and $\Delta n = n_{bs} - n_o$. The low-frequency dielectric constant ε is usually measured by applying a small voltage (~ 0.5 V) to the sample. The polarization contribution to ε is given by $\varepsilon_P = \delta P/(\varepsilon_0 \delta E)$.

At any temperature in the SmAP_{Fmod} range, the parameters m_{ep} and P_{ep} increase with E_{lc} which has a favorable orientation (signified by the suffix ep, the left-side stripe in Fig. 1), and jump to higher values when the field is sufficiently strong to shift the transition to the uniform phase to the given temperature [Figs. 4(a) and 4(b)].
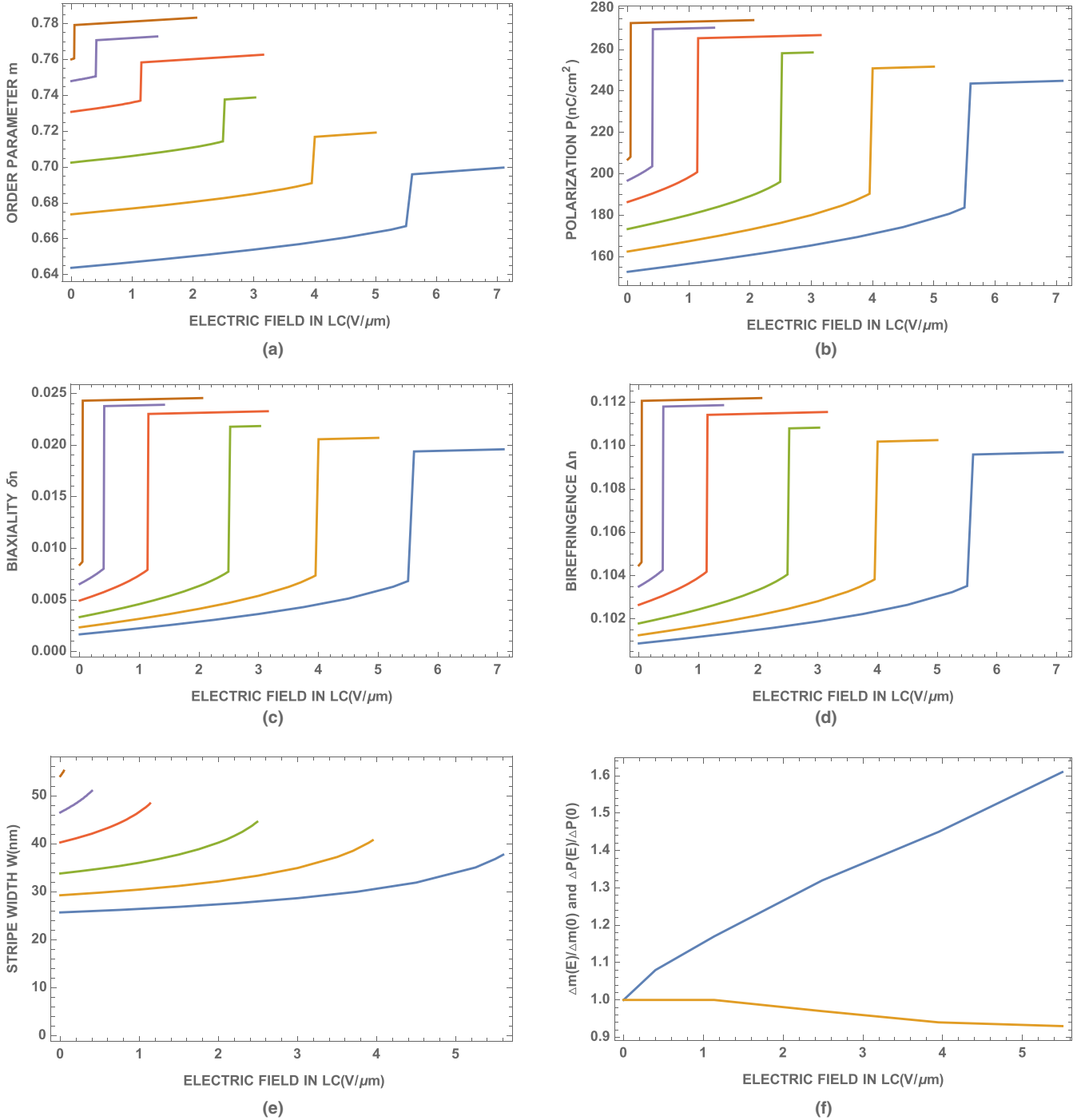
FIG. 4. Variations of different parameters with the dc electric field (E_{lc}) acting on a sample poled along the positive y axis (see Fig. 1). In each figure, the curves correspond, from bottom to top, to the following relative temperatures ($T - T^*$): -65, -70, -75, -80, -83, and -85 K, respectively. The jumps in the curves correspond to the SmAP_{Fmod} to SmAP_{F} transition temperature (T_{tr}) which shifts to a higher temperature with E_{lc}, the relative change in T_{tr} decreasing at higher temperatures. The parameters are (a) order parameter m, (b) polarization P, (c) biaxiality δn, (d) birefringence Δn, and (e) stripe width w, all of which increase with electric field at a given temperature in the stripe phase. The relative jumps at the fields corresponding to the stripe to uniform transition in the order parameter $\Delta m(E)/\Delta m(0)$ with $\Delta m(0) = 0.019$, which is the upper curve in (f), increase significantly with field, whereas that in polarization $\Delta P(E)/\Delta P(0)$ with $\Delta P(0) = 64$ nC/cm^2, which is the lower curve in (f), shows a small decrease.

The positive slope of the variation of T_{tr} with E_{lc} becomes smaller at higher fields. But remarkably, the jump in m at T_{tr} increases at higher E_{lc} [Fig. 4(f)]. On the other hand, the jump in polarization P decreases slightly with E_{lc} [Fig. 4(f)].

From Fig. 4(b) it may also be noted that the polarization contribution to the dielectric constant ($\propto \delta P/\delta E$) increases with E_{lc} in the stripe phase, and becomes quite small in the uniform phase. The field dependences of the biaxiality
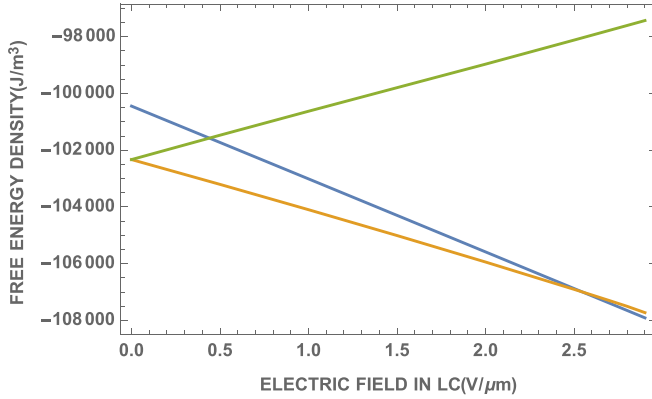
FIG. 5. Electric field dependence of free energy density minimum $\langle F \rangle_m$ in the SmAP$_{Fmod}$ and SmAP$_F$ phases at the relative temperature $T - T^* = -75$ K. At zero field, $\langle F \rangle_m$ is lower in the SmAP$_{Fmod}$ phase, and has a negative slope as a function of E_{lc} for both SmAP$_F$ (topmost curve at $E_{lc} = 0.2$ V/μm) and the stripe phase with m parallel to $\mathbf{E_{lc}}$ on average (bottom-most curve at $E_{lc} = 0.2$ V/μm), as in the left half of Fig. 1. It has a positive slope (middle curve at $E_{lc} = 0.2$ V/μm) when the two vectors point in opposite directions (as in the right half of Fig. 1).

(δn) and the birefringence (Δn) at different temperatures are shown in Figs. 4(c) and 4(d), respectively. The biaxiality remains very low in the stripe phase, as was found experimentally using homeotropically aligned samples, but jumps to a relatively high value at the transition to the uniform phase. The *measured* birefringence exhibits a rapid variation around the transition [21], rather than a sharp jump as in Fig. 4(d). The reason for this difference will be discussed later. The stripe width also increases with E_{lc}, the slope tending to increase as the transition field is approached [Fig. 4(e)].

Experimentally it was found that in the low-temperature SmAP$_F$ phase, the polarization peak occurs at $E = 0$, showing that the projection of $\mathbf{P}$ follows the field. On the other hand, in the SmAP$_{Fmod}$ phase the polarization peak occurs at a temperature dependent threshold field, implying that when the sign of the field is reversed, the stripe structure exhibits a local minimum in free energy. In Eqs. (1) and (2), when the field acts in a direction opposite to the mean $\mathbf{P}$ direction, the last term has a positive sign. Following the same procedure as in the case when that term has a negative sign, the only change is that the $\xi_r^2 \cos\varphi$ term in Eq. (7) also changes sign. Indeed numerical calculations show that the stripe structure has a *local* minimum in the free energy when the field is oriented in the unfavorable direction (as in the right-side stripe in Fig. 1 when $\mathbf{E_{lc}}$ acts along the $+y$ direction). The parameters w_{en}, m_{en}, and P_{en} decrease with E_{lc} with an unfavorable orientation (signified by the suffix en). The distribution of the m-vector across the stripe shifts towards higher φ angles.

The free energy minima as functions of E_{lc} are illustrated for the stripe phase when the field acts in both the orientations, as well as for the uniform phase, at $T^* - T = 75$ K (Fig. 5). At zero field, the stripe phase has a lower free energy compared to the uniform phase. As E_{lc} is increased, the free energies of both the stripe phase with favorable orientation and the uniform phase decrease linearly with field. On the other hand, as expected, the free energy of the stripe phase
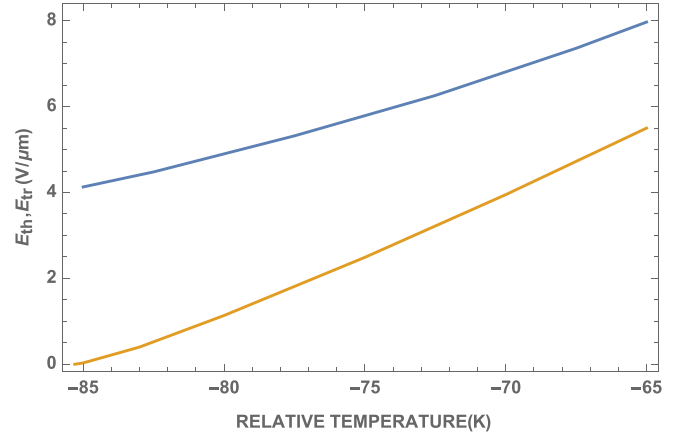

FIG. 6. Threshold electric field E_{th} at which the stripe structure overcomes a barrier to switch from the unfavorable orientation, with average m oriented opposite to $\mathbf{E_{lc}}$, to the favorable orientation (upper curve). For the parameters used in the calculations, it switches to the SmAP$_F$ phase, which has the lowest $\langle F \rangle_m$ value at the threshold field. For comparison, the temperature dependence of the field E_{tr} required for the transition from the stripe to the uniform phase of a *poled* sample is shown in the lower curve.

increases with field which is in the unfavorable orientation, becoming larger than that of the uniform phase at a low value ($\sim$0.45 V/μm) of the field. The uniform phase has the lowest free energy beyond some higher value ($\sim$2.6 V/μm) of E_{lc}. The unfavorable stripe structure can gain energy by changing the structure from that shown in the right side to that in the left side in Fig. 1. This requires a considerable rearrangement, which has to cross a barrier. The peak in the barrier can be expected to occur when $\varphi = \mp\pi/2$, with the free energy density taking a very simple form:

$$F\left(\frac{\pi}{2}\right) = \frac{a}{2}(T - T^*)m^2 + \frac{b}{4}m^4 + \left(\frac{p^2 m^2}{2\varepsilon_0 \varepsilon}\right). \quad (11)$$

The barrier height is given by $\Delta F = F(\pi/2) - \langle F_{en} \rangle$, where the second term is the free energy density averaged over the stripe width when the electric field has the unfavorable orientation. The enhancement of the positive polarization self-energy at $\varphi = \pi/2$ creates the barrier. As the change in structure to the favorable configuration involves the collective reorientation of a large number of molecules, and ΔF is an energy density, it is reasonable to assume that $\Delta F w_{en}^3$ should be comparable to the thermal energy $k_B T$ for the restructuring of the m profile. Indeed as E_{lc} is increased, $\Delta F w_{en}^3$ decreases, and using the criterion mentioned above, at a threshold field (E_{th}) the average $\mathbf{P}$ reverses sign to align with the field. Curiously, at E_{th} the uniform phase has the lowest free energy, and the polarization current peak would correspond to the sum $P_{en} + P_u$, and the measured polarization would be half this value. We show the temperature dependence of E_{th} in Fig. 6. E_{th} has a nonzero value ($\sim$4 V/μm) at the field-free T_{tr}, and increases with temperature, in qualitative agreement with the experimental trend [21]. For comparison, we have also plotted in Fig. 6 the temperature dependence of the transition field E_{tr} of a *poled* sample, derived from the data in Fig. 4.

The experimental studies are conducted on relatively thin (approximately a few micrometers) samples, and moreover the ITO coated plates which are used to apply electric fields are covered with ∼10-nm-thick insulating layers (ILs) to get the required alignment of the sample (see Fig. 1). The latter have a profound influence on the electro-optic (EO) response of ferroelectric liquid crystals with a large polarization **P**, which points in the plane of the layers when the applied electric field is zero, to prevent a large electrostatic energy cost in the liquid crystal and IL due to the field generated by the component of **P** orthogonal to the plates of the cell [22]. The result is a polarization peak and a V-shaped EO response centered at $E = 0$. This is also the response found in the SmAP_F phase [21]. The average value of **P** in the stripe phase is quite large, and as such IL can be expected to influence the electrical response of the medium. As shown in [22], if V_{apl} is the voltage applied to the cell, the voltage drop in the polarized liquid crystal is given by

$$V_{lc} = V_{apl} \pm \frac{2d_{il}}{\varepsilon_0 \varepsilon_{il}} P \cos \varphi, \qquad (12)$$

where d_{il} is the thickness of each insulating layer and ε_{il} its relative dielectric constant. The positive (negative) sign applies when the electric field is opposite to (along) the average polarization direction, as in the right (left) side of Fig. 1. The thickness of the liquid crystal sample d_{lc} is usually a few micrometers, which is much larger than a typical width of the stripe, $w \sim a$ few tens of nanometers. As such, we can use the coarse-grained value $\langle P \cos \varphi \rangle$ in the above equation. The field acting in the liquid crystal E_{lc} used in our theoretical analysis described earlier can now be related to the applied electric field E_{apl} as $E_{lc} = E_{apl} \pm \zeta \langle P \cos \varphi \rangle$, where the constant $\zeta = 2d_{il}/(d_{lc}\varepsilon_0\varepsilon_{il})$ depends on the parameters of the cell, including the gap d_{lc}. Using the width of the polarization peak in the SmAP_F phase reported in [21], we estimate $\zeta \approx 5 \times 10^8$. The threshold of *applied field* for repolarization in such a cell will be ∼1 V/μm lower than that shown in Fig. 6. For comparison with experiment, we have redrawn Fig. 4(d) to show the calculated birefringence Δn as a function of E_{apl} in the favorable orientation (Fig. 7). The polarization jumps at the first order SmAP_{Fmod} to SmAP_F transition at some E_{lc}. The applied field would be larger than E_{lc}, and further, unlike in Fig. 4(d), there is a shift in the corresponding E_{apl} values in the two phases, as P is larger in the uniform phase. The finite slope of the variation of Δn with E_{apl} at this transition signifies a two-phase region, where the stripe and the uniform phases coexist. From Fig. 7, this range extends typically over ∼0.3 V/μm, whereas the experimental range of the spread is ∼3 V/μm [21]. Further, as P jumps down by ∼60 nC/cm^2 across the uniform to stripe phase transition, a narrow coexistence would not have smeared out a current peak heralding the transition, though the event is not seen in the polarization current measurement [21]. We will suggest a plausible explanation of these observations later.

It is clear from Eq. (12) that even when $E_{apl} = 0$, a polarization generated field acts in the liquid crystal, giving rise to an unfavorable positive self-energy. This can be prevented if neighboring stripes orient in opposite directions at zero applied field, as shown in Fig. 1. In such a structure, the net
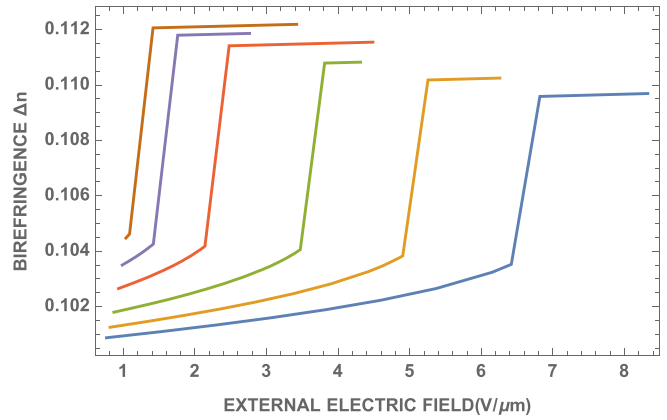

FIG. 7. Birefringence variations shown in Fig. 4(d) redrawn as functions of the applied (external) field E_{apl}, which is higher than the field E_{lc} experienced by the medium, due to an opposing field generated by the polarization, as described in the text. Note that the transition between the two phases has a finite slope, signifying a coexistence of the phases.

polarization and hence the corresponding field would be zero in the coarse-grained model used above. The rearrangement has to cross a large barrier (∼10 $k_B T$), and the Arrhenius process takes a relatively long time. Indeed experimentally it was found that after a waiting period of ∼100 s at zero field, the first repolarization peak in a 4-μm-thick cell amounted to about half the value of P which was obtained in subsequent cycles without a waiting period. The halved signal would be expected from the proposed disposition of neighboring stripes (Fig. 1). This result again shows that the polar anchoring at the surface of the insulating layer is quite weak in the studied compound. The order parameter m, biaxiality δn, and birefringence Δn of the rested sample at zero field would be the same as those calculated earlier [Figs. 2, 4(c), and 4(d)]. However, their dependences on a dc field below the threshold value E_{th} can be expected to be different compared to those of a *poled* sample. The response of the antiparallel neighboring stripes to the field would be different, and the spatially averaged variations with the applied field of the order parameter of such a structure are shown at three temperatures in Fig. 8(a). As expected, the variations are smaller than for a poled sample, shown in Fig. 4(a).

The variations of the average polarization of the antiparallel structure with applied field are shown in Fig. 8(b) at three temperatures. Starting from 0 at $E_{apl} = 0$, the polarization increases rapidly with E_{apl}. Unlike in the usual ferroelectric liquid crystals, a dc bias *increases* the polarization contribution to the dielectric constant, which is proportional to the slope of the curves in Fig. 8(b).

As mentioned earlier, the experimental measurement of variation of Δn with electric field points to a relatively wide spread (∼3 V/μm) in the transition region between the uniform and stripe phases [21]. Following the experimental protocol, we assume that initially a large positive field (**E**$_{max}$) is applied, with **P** oriented along **E**$_{apl}$. At lower temperatures the field is larger than that needed for the transition to the SmAP_F phase, and we can then expect that the excited state conformers spread across the top plate of the cell [Fig. 9(a)],
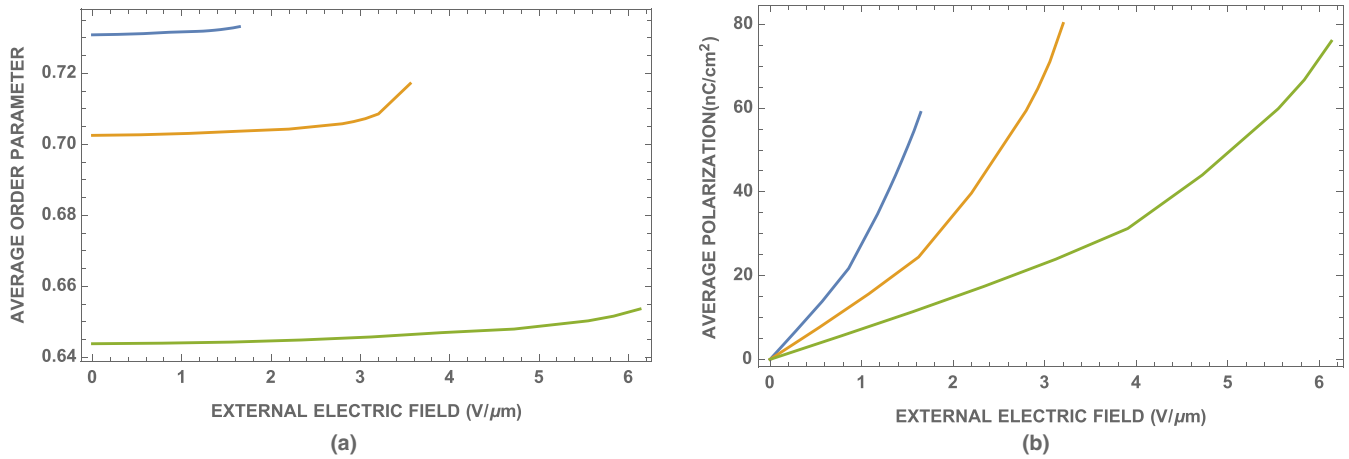
(a)

(b)

FIG. 8. The SmAP$_{\text{Fmod}}$ phase can be expected to have an antiparallel orientation of neighboring stripes when E_{apl} is reduced to 0, and the cell rested for a minute or so, to avoid the positive self-energy due to polarization of a poled structure. This configuration is maintained until the external field reaches the threshold value for the switching of the unfavorably oriented stripes. (a) E_{apl} dependences of the order parameter m averaged over the widths of both types of stripes are shown at $T - T^* = -65$ K (bottom-most curve), -75 K (middle curve), and -85 K (topmost curve). The variations with field are smaller than those in a poled sample, shown in Fig. 4(a). (b) Applied field dependence of the polarization at three temperatures. Note the relatively small value of P, which rapidly rises with E_{apl}. The polarization contribution to the dielectric constant which is $\propto$ to the slope of the curve increases with E_{apl}, unlike in the SmAP$_{\text{F}}$ phase.

effectively increasing the thickness of the insulating layer at that surface. As the field is lowered towards the transition, the mechanism discussed earlier would kick in, with a div**P**-type fluctuation aided by an exodus of ES conformers from the top surface as shown in Fig. 9(b), to lower the free energy. The length scale of the distortion is $\sim \xi_{ep}$ defined after Eq. (7), and the barrier between the two phases depends on the α and β terms of the free energy density. For a volume $\sim \xi_{ep}^3$, the barrier height is of the order of the thermal energy. However, the nucleation of many such walls made of ES conformers and the formation of a periodic structure of the resulting stripes

spanning the entire gap of the cell requires a finite time. If the wall has to span the entire cell gap by a diffusive motion of the ES conformers, the time required is $\sim d_{lc}^2/D$, where d_{lc} is the cell gap and D the diffusion coefficient. For a typical cell gap of 10 μm and $D \sim 10^{-9}$ m^2/s, the wall takes $\sim$0.1 s to reach the opposite end of the cell. For an appropriate combination of the cell gap and the frequency of the triangular voltage, during a considerable fraction of the time required for E to reduce from $E_{\max}$ to zero, the two phases coexist. In the experiments reported in [21], both the birefringence Δn, and polarization current measurements were made using a frequency which was low, but not ultralow as needed for equilibrium measurements. Thus the coexistence range of the two phases would have spread over a relatively large fraction of the period of the time varying electric field. This also means that the polarization current would not show the bump corresponding to the 60 nC/cm^2 difference in the **P** values between the two phases, but would just add to the background current, as in the case of Fig. S2 of the Supplementary Material of Ref. [21], in which the frequency used was 14 Hz. Indeed at lower temperatures, as the field-free transition point is approached, the coexistence of the two phases is directly seen as two separate polarization peaks corresponding to the two phases. The observation of the two peaks over a wide temperature range (about 8 K), though the transition is thermodynamically very weak (with a heat of transition $\sim$60 J/mole) can be understood on the basis of this physical process. The portion of the sample in SmAP$_{\text{F}}$ phase would show the peak centered at $E = 0$, but the portion in the SmAP$_{\text{Fmod}}$ phase, probably sticking out from one plate of the cell, will be trapped in the local minimum of free energy as described earlier, until E_{th} is reached. As both E_{th} and E_{tr} increase with temperature (Fig. 6), for a given amplitude of the triangular voltage, the uniform phase may not grow large enough to survive until E is reduced to zero in a cycle as the temperature is increased beyond some limit
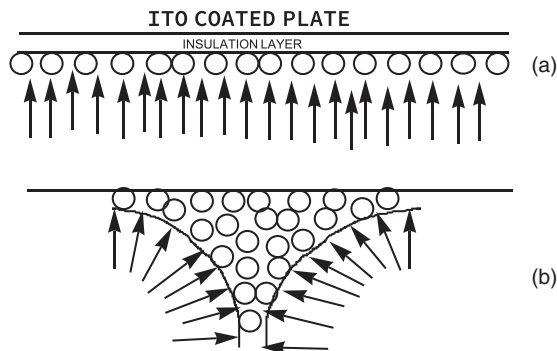

FIG. 9. (a) Schematic diagram showing the likely collection of the ES molecules (which do not exhibit a spontaneous polarization) near the negative electrode when the GS conformers exhibit the SmAP$_{\text{F}}$ phase, stabilized by a large enough E_{apl}. As the field is reduced towards the value at which the SmAP$_{\text{Fmod}}$ phase has the lower free energy, div**P** fluctuations involving a redistribution of the ES molecules as shown in (b) can be triggered. The process of covering the entire cell with the stripe structure with optimum stripe width can take about 0.1 s, and a faster field cycling can lead to a broad coexistence range as seen in experiments [21].

(in the experiment reported in [21], it was about 8 K above the zero field transition temperature). In the birefringence measurements, the maximum applied field (E_{max}) appears to be smaller than E_{tr} beyond some temperature [21].

The small angle x-ray scattering studies detected a few peaks which were not just those arising from one periodic stripe pattern, and could not be indexed to any two-dimensional (2D) lattice [21]. The authors suggested that in the powder sample used, the stripe width may depend on the layer curvature. There can be an additional contribution in view of the model proposed in this paper, as our calculations pertain only to the width (w) of the domains with nonzero order parameter m, whereas the x-ray measurement corresponds to the sum of the widths of the ordered and the disordered (wall) moieties ($w + v$). The ES conformers, and any other impurities in the sample can be expected to have a greater concentration in the more curved parts of the focal conic domains, widening the wall and hence increasing the measured stripe width, compared to the regions with flat layers. Indeed the scattering corresponding to the largest width did not exhibit any harmonic signal, while the ones with smaller spacings (belonging to the flatter layers, and hence better organized) did so. We also note that we have assumed a very strong anchoring of **P**, oriented normal to, and pointed towards the interface. In principle, the anchoring energy can be finite, with both polar and nonpolar contributions, as was assumed in the analysis of the optical data in Ref. [21]. The samples used in experiments can be expected to have ionic impurities whose response to an applied field contributes to the measured properties. As noted in [21], both the concentration and mobility of such impurities increase with temperature, more effectively screening the applied field. Further, our assumption of only two terms of the Landau free energy [with quadratic and quartic dependences on m in Eq. (1)] at temperatures far below T^* is perhaps an oversimplification. As such, only the qualitative trends predicted by our theoretical calculations, which do not take into account the ionic contribution, can be compared with the experimental data.

IV. CONCLUSIONS

In conclusion, we have developed a phenomenological model to describe the stripe (SmAP_{Fmod}) phase and its transition to the uniform (SmAP_F) phase exhibited by bent-core molecules. Following our earlier description of the nematic phase made of BC molecules [24], we assume that while the ground state BC molecules have a polar packing in smectic-A layers, a small fraction of the molecules in an excited state are less bent, and are relatively free to rotate about their bow axes. The latter can aggregate for gaining rotational entropy and form walls, the polarized domains between the walls developing a splay-bend distortion of the polar vector field to lower the energy. The calculations using the model lead to the following results: (1) The stripe width is approximately a few tens of nanometers, increasing as the temperature approaches the transition mentioned above. (2) The order parameter has a small jump at the transition, which is very weakly first order in nature. (3) The average polarization and the main birefringence have relatively large jumps at the transition point. (4) The transition point increases with an applied dc electric field, but exhibits a relatively large range of coexistence. (5) The repolarization current peak occurs at a threshold field in the SmAP_{Fmod} phase, which increases with temperature. (6) In rested samples taken in cells whose plates are coated with insulating layers, neighboring stripes have antiparallel orientations to avoid a positive polarization self-energy. All these results agree qualitatively with the experimental trends found in Ref. [21]. We have also presented results on layer biaxiality, and the influence of a dc field on the properties of rested cells. In particular, a dc bias *increases* the polarization contribution to the dielectric constant in the stripe phase, a trend which is opposite to that in the usual ferroelectric liquid crystals. Hopefully, the SmAP_{Fmod} phase will be found in some other bent-core mesogens to test the predictions of the model. The model may also be applicable to the B_7 phase exhibited by several BC compounds, in which the molecules are tilted rather than being upright in the layers.

[1] R. B. Meyer, L. Liebert, L. Strzelecki, and P. Keller, J. Phys. Lett. **36**, 69 (1975).

[2] T. Niori, T. Sekine, J. Watanabe, T. Furukawa, and H. Takezoe, J. Mater. Chem. **6**, 1231 (1996).

[3] D. R. Link, G. Natale, R. Shao, J. E. Maclennan, N. A. Clark, E. Korblova, and D. M. Walba, Science **278**, 1924 (1997).

[4] B. K. Sadashiva, R. Amaranatha Reddy, R. Pratibha, and N. V. Madhusudana, Chem. Commun. 2140 (2001).

[5] R. Amaranatha Reddy and B. K. Sadashiva, J. Mater. Chem. **14**, 310 (2004).

[6] A. Eremin, S. Diele, G. Pelzl, H. Nadasi, W. Weissflog, J. Salfetnikova, and H. Kresse, Phys. Rev. E **64**, 051707 (2001).

[7] H. Takezoe and A. Eremin, *Bent-Shaped Liquid Crystals* (CRC Press, Boca Raton, FL, 2017).

[8] A. Roy and N. V. Madhusudana, Europhys. Lett. **39**, 335 (1997).

[9] R. Bruinsma and J. Prost, J. Phys. II France **4**, 1209 (1994).

[10] L. Guo, E. Gorecka, D. Pociecha, N. Vaupotic, M. Čepič, R. Amaranatha Reddy, K. Gornik, F. Araoka, N. A. Clark, D. M.

Walba, K. Ishikawa, and H. Takezoe, Phys. Rev. E **84**, 031706 (2011).

[11] R. Amaranatha Reddy, C. Zhu, R. Shao, E. Korblova, T. Gong, Y. Shen, E. Garcia, M. A. Glaser, J. E. Maclennan, D. M. Walba, and N. A. Clark, Science **332**, 72 (2011).

[12] E. D. Korblova, E. Guzman, J. E. Maclennan, M. A. Glaser, R. Shao, E. Garcia, Y. Shen, R. Visvanathan, N. A. Clark, and D. M. Walba, Materials **10**, 1284 (2017).

[13] D. Blankschtein and R. M. Hornreich, Phys. Rev. B **32**, 3214 (1985).

[14] G. A. Hinshaw, Jr., and R. G. Petschek, Phys. Rev. B **37**, 2133 (1988).

[15] A. E. Jacobs, G. Goldner, and D. Mukamel, Phys. Rev. A **45**, 5783 (1992).

[16] D. A. Coleman, J. Fernsler, N. Chattam, M. Nakata, Y. Takanishi, E. Korblova, D. R. Link, R. F. Shao, W. G. Jang, J. E. Maclennan, O. Mondainn-Monval, C. Boyer, W. Weissflog, G. Pelzl, L. C. Chien, J. Zasadzinski, J. Watanabe, D. M.

Walba, H. Takezoe, and N. A. Clark, Science **301**, 1204 (2003).

[17] M. Nakata, D. R. Link, Y. Takanishi, Y. Takahasi, J. Thisayukta, H. Niwano, D. A. Coleman, J. Watanabe, A. Iida, N. A. Clark, and H. Takezoe, Phys. Rev. E **71**, 011705 (2005).

[18] D. A. Coleman, C. D. Jones, M. Nakata, N. A. Clark, D. M. Walba, W. Weissflog, K. Fodor-Csorba, J. Watanabe, V. Novotna, and V. Hamplova, Phys. Rev. E **77**, 021703 (2008).

[19] N. Vaupotic and M. Copic, Phys. Rev. E **72**, 031701 (2005).

[20] N. Vaupotic, Ferroelectrics **344**, 151 (2006).

[21] C. Zhu, R. Shao, R. Amaranatha Reddy, D. Chen, Y. Shen, T. Gong, M. A. Glaser, E. Korblova, P. Rudquist, J. E. Maclennan, D. M. Walba, and N. A. Clark, J. Am. Chem. Soc. **134**, 9681 (2012).

[22] N. A. Clark, D. Coleman, and J. E. Maclennan, Liq. Cryst. **27**, 985 (2000).

[23] A. Jakli, Liq. Cryst. Rev. **1**, 65 (2013), and references therein.

[24] N. V. Madhusudana, Phys. Rev. E **96**, 022710 (2017).

[25] T. Ostapenko, D. B. Wiant, S. N. Sprunt, A. Jakli, and J. T. Gleeson, Phys. Rev. Lett. **101**, 247801 (2008).

[26] K. S. Krishnamurthy, M. B. Kanakala, C. V. Yelamaggad, and N. V. Madhusudana, J. Phys. Chem. B **123**, 1423 (2019).

[27] M. Nakagawa, M. Ishikawa, and T. Akahane, Jpn. J. Appl. Phys. **27**, 456 (1988).

[28] M. H. Lu, K. A. Crandall, and C. Rosenblatt, Phys. Rev. Lett. **68**, 3575 (1992).

[29] D. R. Link, N. Chattham, J. E. Maclennan, and N. A. Clark, Phys. Rev. E **71**, 021704 (2005).

[30] J. B. Lee, D. Konovalov, and R. B. Meyer, Phys. Rev. E **73**, 051705 (2006).

[31] M. Copic, J. E. Maclennan, and N. A. Clark, Phys. Rev. E **65**, 021708 (2002).